Published in final edited form as:
J Immunol. 2013 November 15; 191(10): . doi:10.4049/jimmunol.1301433.

Selective Activation of Antigen-Experienced T Cells by Anti-CD3 Constrained on Nanoparticles

Ying-Chun Lo[*], **Michael A. Edidin**[†,‡], and **Jonathan D. Powell**[*,§]

[*] Department Pharmacology and Molecular Sciences, School of Medicine, Johns Hopkins University, Baltimore, Maryland, USA.

[†] Department of Biology, Zanvyl Krieger School of Arts and Sciences, Johns Hopkins University, Baltimore, Maryland, USA.

[‡] Department of Materials Science, Whiting School of Engineering, Johns Hopkins University, Baltimore, Maryland, USA.

[§] Department of Oncology, School of Medicine, Johns Hopkins University, Baltimore, Maryland, USA.

Abstract

Activation of T cells through the T cell receptor (TCR) is mediated by the TCR-CD3 signaling complex. Cross linking of this complex with antibodies directed against CD3 leads to potent activation of T cells. However, such activation is not antigen-specific. We exploited the observation that the TCR-CD3 complex is clustered on T cells that have been activated by antigen by using anti-CD3 nanoparticles to selectively activate antigen-experienced mouse T cells. We find that constraining anti-CD3 on the surface of a nanoparticle markedly and selectively enhances proliferation and cytokine production of antigen-experienced T cells but does not activate naïve T cells. This effect was recapitulated in heterogeneous cultures containing mixtures of antigen-specific CD4+ or CD8+ T cells and bystander T cells. Furthermore, *in vivo* anti-CD3 coated nanoparticles increased the expansion of antigen-specific T cells following vaccination. Overall, these findings indicate that anti-CD3 coated nanoparticles could be use to enhance the efficacy of vaccines and immunotherapy. The results also suggest constraining a ligand on the surface of a nanoparticle might as general strategy for selectively targeting clustered receptors.

Introduction

Specificity and memory are key features of the adaptive immune system (1, 2). An adaptive immune response amplifies a small population of antigen-specific B and T lymphocytes to promote the clearance of an infection. While B cell receptors (antibodies) can recognize soluble intact antigen, T cells recognize cognate peptides presented in the context of MHC molecules on the surface of antigen presenting cells (APCs) (3). On naïve T cells, the antigen-specific T cell receptor (TCR) is distributed across the surface of the cell in nanoclusters; these nanoclusters oligomerize into micro-clusters after T cells are activated by antigen (4-6). Clustering promotes the transmission of intracellular signals via the CD3 signaling complex leading to T cell activation (7-10). It is also believed to increase the sensitivity for low concentrations of antigen (11) and to generate maximal local signals by providing continuous engagement of TCR/MHC (12). TCR microclusters are observed in

Address correspondence and reprint requests to Dr. Jonathan D. Powell, Department of Oncology, School of Medicine, Johns Hopkins University. Cancer Research Building 1, Room 443, 1650 Orleans Street, Baltimore, Maryland, 21231, USA. Tel: 410-502-7887, Fax: 410-614-9705 poweljo@jhmi.edu.

both effector and memory cells; their presence correlates with increased sensitivity of antigen-experienced T cells (13).

It has been estimated that the number of TCRs within a nanocluster, prior to activation, ranges from a single receptor to a cluster of 20 or more (11). Binding experiments indicate that these clusters are 1-3 nanometers in size (5). On the other hand, microclusters, which are formed upon T cell activation, have been estimated to be hundreds of nanometers in diameter (14, 15) and contain approximately 100 TCR complexes as determined by total internal reflection fluorescence microscopy (16). Furthermore, by employing photo-activated localization microscopy, density domains inside microclusters have been estimated to be 35-70 nm in diameter and contain 7-20 TCRs (17). Based on such data, it is reasonable to assume that the distance between two TCR complexes in the micro-cluster of activated T cells is about 20 nm.

We hypothesized that the difference in TCR clustering between naïve and recently activated T cells could be exploited in order to selectively boost antigen-specific responses. To test our hypothesis we used mAb to CD3, a general T cell activator, bound to quantum dots (QD) (14, 18-20). Anti-CD3 coated Qdots® 605 (anti-CD3 QD; Invitrogen) are about 18 nm in diameter and are coupled to multiple anti-CD3 antibodies, which are potent T cell agonists. In this report we demonstrate that anti-CD3 constrained on the surface of a nanoparticle selectively activates only T cells that are antigen experienced and, in contrast to soluble anti-CD3, does not activate naïve T cells.

Materials & Methods

Microscopy

Cells were fixed by 2% formaldehyde, stained with rabbit anti-mouse CD3-γ (Santa Cruz) for overnight and goat anti-rabbit DyLight 488 (Jackson ImmunoResearch) for 2 hours. Cells were then mounted with Prolong Gold Anti-fade reagent (Invitrogen) and imaged with an upright fluorescence microscope with 710NLO-Meta confocal module (AxioExaminer; Zeiss) with a 63x /1.2W C-Apo objective. Microclusters were identified using the “Find objects using intensity (>21044)” and “Separate touching objects (object size guide 0.08 μm^2)” functions of Volocity imaging analysis software. Data were acquired with Zen imaging software (Zeiss) and analyzed with Volocity analysis software (PerkinElmer).

Mice

Mice were kept in accordance with guidelines of the Johns Hopkins University Institutional Animal Care and Use Committee. 5C.C7 TCR transgenic RAG2−/− mice and DO11.10 TCR transgenic RAG2−/− mice [Thy1.2+, K^d; HA-specific] were from Taconic Farms. 6.5 TCR transgenic [Thy1.1+, K^d; HA-specific] mice, B10.D2 [Thy1.1+, K^d] mice, clone 4 TCR transgenic [Thy1.1+, K^d; HA-specific] mice, OT-1 TCR transgenic RAG2−/− [Thy1.1+, K^b; HA-specific] mice, and B10.D2 [Thy1.2+, K^d] mice were a gift from Charles Drake. C57BL/6 [Thy1.2+, K^b] mice were obtained from Jackson Laboratories.

Reagents and Antibodies

Hamster anti-mouse CD3 (145-2C11) Qdot® 605 and Qdot® 655 streptavidin conjugate were purchased from Invitrogen. Antibodies against the following proteins were purchased from BD Biosciences: CD4 (GK1.5), CD8a (53-6.7), Thy1.1 (OX-7), Thy1.2 (53-2.1), Vβ8.1/8.2 (MR5-2), IFN-γ (XMG1.2), and IL-4 (11B11). Biotin-labeled antibodies against 6.5 TCR and stimulatory anti-CD3 (145-2C11) antibodies as well as neutralizing anti-IL-4 (11B11) and anti-IFN-γ (XMG1.2) antibodies were purified from hybridoma supernatants prepared ‘in-house’. Neutralizing anti-IL-12p40 (C17.8) antibodies were from eBioscience.

Other regents used: CFSE cell proliferation kit (Invitrogen), eFluor® 670 cell proliferation dye (eBioscience), fluorophore conjugated streptavidin (BD Biosciences), IL-2, IL-7, IFN-γ, IL-12 p40, and IL-4 cytokines (all from Pepro Tech), PCC protein and OVA protein (Sigma -Aldrich), HA class II peptide (SFERFEIFPKE), HA class I peptide (IYSTVASSL)(both from Johns Hopkins Synthesis and Sequencing Facility), OVA class II peptide (ISQAVHAAHAEINEAGR), OVA class I peptide (SIINFEKL) (both from AnaSpec), and Imject® Freund's Complete Adjuvant (Thermo Scientific).

Flow Cytometry and Intracellular staining

All experiments were performed on a BD Calibur and analyzed using FlowJo analysis software. Brefeldin A (GolgiPlug) or monensin (GolgiStop) was used for cytokine staining. Cells were surface stained, underwent Fixation/Permeabilization followed by staining for intracellular proteins in Perm/Wash Buffer (reagent all from BD Biosciences). Gates were set appropriately with un-stimulated and controls. Voltages were determined from un-stained controls.

Proliferation and ELISA

Proliferation was measured by dilution of CFSE or eFluor 670 cell proliferation dyes. Cells were labeled according to the manufacturer's protocol. The cytokines IFN-γ and IL-4 were measured in supernatants by ELISA as described by the manufacturer (eBioscience).

Cell Culture

Unless otherwise stated, splenocytes were cultured in 50% RPMI/50% EHAA media supplemented with 10% heat-inactivated low-LPS FBS, 1% penicillin/streptomycin, and 1% glutamine. APCs were from the non-CD4+, column-bound fraction of CD4+ T cell isolation. For T_H1 and T_H2 cultures, splenocytes were stimulated in media supplemented with 5 μM PCC and different skewing cytokines and antibodies for 48 h. Skewing conditions were as follows: T_H1, IL-12 (5 ng/ml), IFN-γ (100 ng/ml) and anti-IL-4 (100 μg/ml); T_H2, IL-4 (1 ng/ml), anti-IL-12 (100 μg/ml) and anti-IFN-γ (100 μg/ml).

Adoptive transfer

For adoptive transfer experiments, 6.5 TCR transgenic mice were sacrificed via CO_2 asphyxiation. Spleens and lymph nodes were collected and homogenized, and red blood cells were lysed. CD4+ T cells were purified using Miltenyi magnetically labeled beads (Miltenyi Biotec) according to the manufacturer's protocol. Cells were then washed and resuspended with PBS for i.v. injections. Typically, 1-5 × 10^6 cells were injected per mouse in 0.2 ml PBS by retro-orbital i.v. injection.

Results

Antigen recognition leads to TCR clustering

Emerging studies reveal that after antigen recognition there is clustering of T cell receptors (TCR) not only at the T cell–antigen presenting cell (APC) interface but also on the whole surface of the T cell (12). We employed confocal microscopy to image the distribution of TCRs on T cells before and after antigen exposure. We imaged 1 μm below the top of the cell, trading off sharpness for the largest area of membrane in a single image. It has been reported that membrane molecules remain mobile after fixation (21) and the observed clustering could be amplified by the antibody used for staining. However, the observed clustering differences between naïve and primed cells are consistent with those on live cells.

Naïve RAG2$^{-/-}$ CD4+ 5C.C7 TCR transgenic T cells, stained for the TCR signaling complex using purified anti-CD3 and Alexa 488 labeled secondary antibody, showed few clusters and a relatively uniform distribution of TCR on the surface (Fig. 1A). After 24 hours of stimulation *in vitro* with 0.05 μM PCC protein we observed the formation of TCR microclusters over the surface of the activated T cells (Fig. 1B). To determine whether these microclusters persisted, 5C.C7 cells stimulated *in vitro* with 0.05 μM PCC protein were then rested in media supplemented with 100 ng/ml IL-2 and 10 ng/ml IL-7 without antigen for another 6 days. At this time point, 6 days after the encounter with antigen the TCR microclusters were still present (Fig. 1C).

To further quantify the numbers of microclusters on T cells, images of at least 25 cells for each condition were collected and microclusters were identified using the Volocity software (Fig. 1D-F). Fresh naïve 5C.C7 cells had an average of 15 microclusters on a single imaging slice. On the other hand, there was a marked increase in the number of microclusters, to an average of 50 per cell, after 24 hours of stimulation. Similarly, after resting for 6 days, we still observed an average of 35 microclusters on the surface of the cells (Fig. 1G). The average area of the microclusters on the activated cells was 0.1255 μm^2. The size of the microclusters decreased to 0.0844 μm^2 after 6 days of rest, however their size remained larger than those observed on the naïve T cells, which was 0.0667 μm^2 (Fig. 1H). The total amount of TCRs expressed on the surface of the naïve and 6-day activated T cells, as determined by mean fluorescence intensity, was similar (Fig. 1I). Thus, while the overall number of TCRs on the surface of naïve and recently activated T cells was similar, the size and intensity of TCR microclusters differentiated antigen-experienced 5C.C7 T cells from naïve cells.

Constraining anti-CD3 antibodies on nanoparticles selectively activates antigen-experienced CD4+ T cells

Soluble anti-CD3 activates all T cells regardless of their antigen specificity by crosslinking the TCR-CD3 signaling machinery (22, 23). We postulated that the different degrees of TCR clustering on the surface of antigen-experienced versus naïve T cells could be exploited to selectively activate only the T cells that had previously engaged antigen (Fig. 2A-B). We reasoned that in general, the cross linking ability of anti-CD3 when constrained to a nanoparticle would be limited when the TCRs were scattered across the surface of the cell, as is the case for naïve T cells, but that the anti-CD3 QD could engage the TCR in the microclusters that develop after T cell activation.

To this end, naïve 5C.C7 splenocytes were incubated *in vitro* with media or PCC protein together with anti-CD3 QD for 72 hours and evaluated for proliferation. T cells that were not previously activated by antigen failed to proliferate in response to the anti-CD3 QD even at the highest concentration, but responded perfectly well to soluble anti-CD3 (data not shown for 5C.C7, but see Fig. 4A for another example). T cells incubated with low dose peptide proliferated modestly, while the addition of anti-CD3 QD resulted in markedly enhanced proliferation. This selective enhancement also increased with increasing amounts of anti-CD3 QD (Fig. 2C). In addition, the ability of the anti-CD3 QD to enhance proliferation was maintained even if we removed the antigen from the culture (Supplemental Fig. 1).

We hypothesize that TCR clustering on the surface of previously activated T cells enables them to be stimulated by the anti-CD3 coated QD. To test this hypothesis, 5C.C7 cells were stimulated with PCC protein for two days and rested in IL-2 and IL-7 for 7 days and then were CFSE labeled and re-stimulated with anti-CD3 QD and fresh APCs. T cells that had seen antigen 6 days earlier proliferated vigorously in response to 1 nM of anti-CD3 QD but did not respond to fresh APCs alone. Also, naïve 5C.C7 cells responded minimally to the

same concentration of anti-CD3 QD (Fig. 2D, Supplemental Fig. 2A). Thus, antigen-experienced T cells, who's TCR are clustered, are responsive to anti-CD3 QD while T cells that have yet to see their antigen (and have most TCR diffusely distributed) are unresponsive.

The ability of anti-CD3 QD to selectively enhance the proliferation of antigen-experienced T cells was antigen-specific. PCC-specific 5C.C7 T cells were incubated with either specific antigen, PCC or with control Ovalbumin (ova) and then assayed for their ability to respond to the anti-CD3 QD. After 72 hours, naïve 5C.C7 cells responded minimally to anti-CD3 QD without the presence of peptide (Fig. 3, Supplemental Fig. 2B). 5C.C7 T cells co-incubated with Ova antigen, failed to respond to 18.5 pM anti-CD3 QD (Fig. 3). In addition, stimulation of antigen-experienced T cells was not a property of un-modified QD, since streptavidin coated QD (SA-QD) lacking anti-CD3 failed to stimulate proliferation of the antigen-experienced 5C.C7 T cells (Fig. 3).

Constraining anti-CD3 antibodies on nanoparticles selectively activates both CD4+ and CD8+ T cells

First, we repeated our experiments with splenocytes from $RAG^{+/+}$ 6.5 TCR transgenic mice. The 6.5 transgenic TCR is specific for Class II hemagglutinin (HA) peptide. However, since these mice are wild type for the RAG gene, only 10-20% of the CD4+ T cells express the transgenic TCR. The remaining cells, that are negative for the transgenic TCR (6.5−), express TCR with other specificities. This allows us to simultaneously evaluate the specificity of anti-CD3 QD for antigen-specific and endogenous T cells in a single culture. We stimulated the splenocytes with HA II peptide for 48 hours followed by the addition of anti-CD3 QD or soluble anti-CD3. Proliferation was analyzed 3 days after addition of anti-CD3 QD. Both 6.5+ and 6.5− T cells proliferated in response to 23 nM soluble anti-CD3 regardless of whether the cells were pre-incubated with HA peptide (Fig. 4A). On the other hand, none of the 6.5+ or 6.5− T cells proliferated in response to 8.7 nM anti-CD3 QD alone, without HA peptide. Low dose HA II peptide, as expected, only stimulated the 6.5+ T cells. The addition of anti-CD3 QD to such cultures led to a marked enhancement of proliferation of the 6.5+ T cells but not of the 6.5− T cells (Fig. 4A). There were similar concentrations of anti-CD3 in both culture conditions: 23 nM in soluble antibody and approximately 45 nM in anti-CD3 QD, assuming there are 5-10 antibodies on a QD (15). Since the amount of anti-CD3 antibodies are similar, the enhancement of activation by anti-CD3 QD does not reflect a large difference in antibody available for cross-linking TCR, but rather the difference between the crosslinking capacity of soluble antibody molecules and that of antibodies constrained onto nanoparticles.

We next tested a second experimental system for the selectivity of anti-CD3 QD in activating antigen-specific CD4+ T cells. Splenocytes from class II OVA specific DO11.10 $RAG2^{-/-}$ (Thy1.2) mice and wild type B10.D2 (Thy1.1) mice, which share the same $H\text{-}2^{d}$ background, were co-cultured with or without class II OVA peptide. Anti-CD3 QD or media was added to the culture one day later for an additional two days. Without the addition of OVA peptide, neither B10.D2 nor DO11.10 CD4+ cells proliferated (Fig. 4B). The addition of class II OVA peptide led to the proliferation of only the antigen-specific DO11.10 cells. The addition of anti-CD3 QD to the OVA treated cultures led to the enhanced proliferation of the DO11.10 T cells but did not stimulate the B10.D2 CD4+ T cells (Fig. 4B).

Clustering of TCRs upon antigen-induced activation has also been shown for CD8+ T cells (16). We found that anti-CD3 coated QD also selectively enhance the activation of CD8+ T cells. $RAG^{+/+}$ CD8+ Clone 4 TCR transgenic T cells, specific for class I HA peptide were stimulated with 10 nM of HA I for 24 hours. Anti-CD3 QD were then added into the culture to a final concentration of 10 nM two days before we harvested the cells. As was observed

with CD4+ T cells, anti-CD3 QD alone did not induce proliferation in the absence of antigen. However, co-culture of HA Class I peptide with the anti-CD3 coated QD led to a marked enhancement of the antigen-specific (Vβ8.2+) CD8+ T cells (Fig. 4C). Thus, anti-CD3 QD could also selectively enhance the activation of antigen-specific CD8+ T cells.

We next tested the ability of anti-CD3 coated QD to selectively enhance CD8+ T cell activation in cultures containing T cells of mixed specificity. T cells from OVA specific RAG2$^{-/-}$ CD8+ OT-1 (Thy1.1+) TCR transgenic mice were mixed with T cells from wild type C57BL/6 (Thy1.2) mice. The cells were cultured with or without class I OVA peptide in the presence and absence of anti-CD3 QD. Anti-CD3 QD alone or media failed to induce T cell proliferation in any of the CD8+ T cells (Fig. 4D). In the presence of class I OVA peptide, only the antigen-specific OT-1 cells proliferated. The addition of anti-CD3 QD to such cultures led to the enhanced activation of the OT-1 CD8+ T cells but not the other CD8+ T cells (Fig. 4D). Thus, anti-CD3 QD have the ability to selectively enhance the activation of antigen-specific CD8+ T cells as well as CD4+ T cells.

Anti-CD3 QD enhance effector generation and function

Thus far we have demonstrated the ability of anti-CD3 QD to enhance the proliferation of CD4+ and CD8+ T cells. We next tested whether the anti-CD3 QD could promote the generation of specific CD4+ effector cells. Splenocytes from CD4+ 6.5 TCR transgenic mice were stimulated *in vitro* with class II HA peptide for 48 hours. Anti-CD3 QD were then added to the culture and cells incubated for another 4 days. In these long-term cultures, the addition of anti-CD3 QD led to an increase in the number of IFN-γ-producing 6.5+ T cells (Fig. 5A). This increase in IFN-g secreting cells was also reflected in the amount of IFN-γ secreted into the supernatant as measured by ELISA (Fig. 5B).

Anti-CD3 QD selectively enhanced effector cell generation under specific Th skewing conditions (Fig. 5C). Naïve 5C.C7 splenocytes were incubated with PCC peptide under conditions that would promote the generation of either Th1 (IFN-γ +IL-12+ anti-IL-4 Ab) or Th2 (IL-4 + anti- IFN-γ Ab+anti-IL-12Ab) effector cells for 2 days. On the third day the cells were incubated with different concentrations of anti-CD3 QD and then assayed for both proliferation and cytokine production. As expected, anti-CD3 QD enhanced the proliferation of antigen-activated T cells in both Th1 and Th2 conditions (Fig. 5D). Furthermore, the addition of the anti-CD3 QD enhanced the production of IFN-γ in the cells activated under Th1 conditions and production of IL-4 in the cells activated under Th2 conditions. Thus, the anti-CD3 QD enhanced both proliferation and cytokine production in antigen-experienced CD4+ effector cells.

Anti-CD3 QD boosts responses to vaccines *in vivo*

Next, we wanted to determine if activation of T cells *in vivo* rendered them susceptible to activation by anti-CD3 QD. We transferred 6.5+ Thy1.1+ CD4+ T cells into WT B10.D2 Thy1.2+ mice, which were then injected with class II HA peptide mixed with CFA. Six days later, draining lymph nodes were harvested. The harvested cells were CFSE labeled and then cultured in media only or with anti-CD3 QD. After three days of *in vitro* restimulation with anti-CD3 QD, we observed that only the 6.5+ CD4+ T cells responded. That is, the anti-CD3 QD only stimulated the lymph node T cells that had previously encountered antigen *in vivo* (Fig. 6A). Both 6.5+ and 6.5− T cells proliferated in positive control cultures, with soluble anti-CD3 (Fig. 6B) and abrogated specificity. Thus, *in vivo* activated antigen-specific T cells were as responsive to anti-CD3 QD to cells that were activated *in vitro*.

Finally, we wanted to determine if anti-CD3 QD could enhance the response to a vaccine *in vivo*. Again 6.5+ Thy1.1+ CD4+ T cells were adoptively transferred into WT B10.D2

Thy1.2+ mice, which were then vaccinated subcutaneously with PBS or class II HA peptide with CFA to generate newly activated 6.5+ T cells. Two days later, mice were injected with PBS or anti-CD3 QD at the same site. Three days later, draining lymph nodes were harvested and the frequency of antigen-specific CD4+ Vβ8.1.2+ cells was evaluated. Treatment with anti-CD3 QD led to an increase in the frequency of vaccine-induced antigen-specific CD4+ Vβ8.1.2+ T cells in the draining lymph nodes compared to the frequency in nodes of animals given PBS (Fig. 6C), but did not lead to widespread activation of endogenous memory T cells (Supplemental Fig. 2C-E). Thus, the sequenced administration of antigen and anti-CD3 QD enhanced the initial vaccine-induced expansion of antigen-specific T cells *in vivo*. To expand these findings we performed a similar experiment to determine if the addition of anti-CD3 QD could enhance the generation of memory cells. Mice were vaccinated with peptide and then injected with PBS or anti-CD3 QD one day later. After an additional 11 days, the mice were infected with vaccinia virus that expresses HA peptide (vaccinia-HA). We observed that mice which received the peptide (day 0) followed by the anti-CD3 QD (day 1) had an increased recall response when challenged with vaccinia-HA administered on day +12 (Fig. 6D). In addition, antigen-specific T cells from the anti-CD3 QD treated mice had higher IFN-γ and IL-2 production than controls (Fig. 6E-F). These results are consistent with the hypothesis that the sequenced administration of antigen and anti-CD3 QD enhance the generation of functional memory cells. These data also argue against the possibility that enhanced proliferation of T cells induced by anti-CD3 QD results in cell death after the initial burst of proliferation.

Discussion

Nanoparticles have been explored for various applications not only because of their miniature size but also because of their relatively large surface area which allows immobilization of multiple ligands (24-26). Owing to these unique physicochemical and functional properties, nanoparticles have been used as carriers for antigen delivery, with successful examples including enhancing the efficacy of dentritic cell-based cancer immunotherapy (24, 27-30). Colloidal semiconductor nanocrystals, often referred to as “quantum dots,” are a new generation of fluorescent dyes with advantage of brightness, photobleaching resistance, good chemical stability, and tunable spectral properties compared to traditional organic fluorophores and fluorescent tagging molecules (15, 16). Antibody conjugated QD were developed for high-resolution labeling and were used to show the co-clustering of TCR and CD4 or CD8 co-receptor in microclusters in recently activated T cells (6, 31). In this report we are able to exploit the unique properties of antibody-coated QD not for imaging but rather to selectively activate antigen-specific T cells.

While soluble anti-CD3 acts as a potent T cell mitogen, activating T cells indiscriminate of TCR specificity (23), we find that anti-CD3 constrained on the surface of a nanoparticle specifically activates antigen-experienced T cells. Thus, by constraining anti-CD3 on the surface of nanoparticles we have imparted selectivity. We hypothesize that this selectivity is due to the fact that, unlike naïve T cells, antigen activated T cells display microclusters of the TCR on their surface (5, 6, 16). TCRs in these clusters are more sensitive to crosslinking by the anti-CD3 coated nanoparticles than are TCR dispersed in smaller clusters across the surface of naïve cells. In support of this hypothesis is our finding that T cells which have been rested for 6 days after antigen stimulation, and still display TCR microclusters, remain sensitive to activation by anti-CD3 coated nanoparticles. In addition, preliminary studies employing (larger) 100 nm CD3-gold particles activated both naïve and antigen-experienced T cells (data not shown). Future studies employing a series of anti-CD3-coated gold particles of varying sizes will better define the relationship between the cluster size and the selective responsiveness to anti-CD3 constrained agonists. Alternatively, it is possible that the ability of anti-CD3 coated nanoparticles to selectively activate antigen-specific T cells is

not due to the differences in microclusters exhibited by activated and resting T cells. It may be that the signaling machinery of previously activated T cells is more sensitive to limited exposure of anti-CD3 than resting T cells. Indeed, the kinetic segregation model suggests that these differences in response to antigen are due to the local changes in the balance of kinases and phosphatases associated with the TCR (32). Thus it is possible that our results are not secondary to clustering *per se*, but rather due to changes in the topography of kinases and phosphatases in the antigen-experienced cells that make them more sensitive to activation when anti-CD3 coated nanoparticles engage TCR.

Our *in vivo* data suggest that anti-CD3 coated nanoparticles could be employed clinically to enhance the magnitude of the response to vaccines for both infectious diseases as well as tumors. *In vivo*, the administration of the anti-CD3 coated nanoparticles enhanced the frequency of the antigen-specific T cells without any evidence of non-specific T cell activation. Such findings suggest that the co-administration of antigen and anti-CD3 coated nanoparticles might lead to the enhancement of the T cell responses. Furthermore, we find that the administration of anti-CD3 coated nanoparticles during the initial encounter with antigen can result in increased generation of memory cells. Indeed, the mice treated with the anti-CD3 coated nanoparticles demonstrated increased recall responses upon rechallenge 10 days later. Such a finding suggests that this strategy might be employed to enhance the efficacy of preventative vaccines by boosting the generation of memory cells.

We believe that our findings have broad implications for promoting specificity even outside of the immune system. The selectivity of receptor-ligand interactions imparts signaling specificity. The specific expression of receptors on different cell types enables biologic selectivity. However, broad distribution of a receptor can present a hurdle to developing pharmacologic agents. The benefits of the specific biochemical pathways blocked or induced by ligand specificity may be mitigated by the fact that receptor is expressed on a diversity of cells. One such example of this is seen in the use of the anti-lymphoma agent anti-CD20 (rituximab) (33). CD20 is expressed on lymphoma cells (34) and indeed, rituximab is efficient at destroying tumor cells. On the other hand the expression of CD20 on all B cells, means that a consequence of treatment is the depletion of non-malignant B cells. If CD20 is clustered on lymphoma cells when compared to normal B cells, it is possible that constraining anti-CD20 on the surface of a nanoparticle might demonstrate greater selectivity for lymphoma cells. That is, constraining a particular ligand on the surface of a nanoparticle may promote the targeted activation of its receptor selectively on the desired cell type.

Supplementary Material

Refer to Web version on PubMed Central for supplementary material.

Acknowledgments

We would like to thank the members of the Powell and Drake Labs for their helpful suggestions and reagent contributions. We thank Dr. Scot Kuo and people in the Johns Hopkins University School of Medicine Microscope Facility for advice confocal microscopy.

This work was supported by National Institutes of Health grants R56AI099276 and P01AI072677.

Abbreviations used in this article

QD	quantum dots
nm	nanometer

References

1. Bonilla FA, Oettgen HC. Adaptive immunity. J Allergy Clin Immunol. 2010; 125:S33–40. [PubMed: 20061006]
2. Litman GW, Rast JP, Fugmann SD. The origins of vertebrate adaptive immunity. Nat Rev Immunol. 2010; 10:543–553. [PubMed: 20651744]
3. Davis MM, Bjorkman PJ. T-cell antigen receptor genes and Tcell recognition. Nature. 1988; 334:395–402. [PubMed: 3043226]
4. Dustin ML, Groves JT. Receptor signaling clusters in the immune synapse. Annu Rev Biophys. 2012; 41:543–556. [PubMed: 22404679]
5. Fahmy TM, Bieler JG, Edidin M, Schneck JP. Increased TCR avidity after T cell activation: a mechanism for sensing low-density antigen. Immunity. 2001; 14:135–143. [PubMed: 11239446]
6. Zhong L, Zeng G, Lu X, Wang RC, Gong G, Yan L, Huang D, Chen ZW. NSOM/QD-based direct visualization of CD3-induced and CD28-enhanced nanospatial coclustering of TCR and coreceptor in nanodomains in T cell activation. PLoS One. 2009; 4:e5945. [PubMed: 19536289]
7. Anikeeva N, Gakamsky D, Scholler J, Sykulev Y. Evidence that the density of self peptide-MHC ligands regulates T-cell receptor signaling. PLoS One. 2012; 7:e41466. [PubMed: 22870225]
8. Fernandez-Miguel G, Alarcon B, Iglesias A, Bluethmann H, Alvarez-Mon M, Sanz E, de la Hera A. Multivalent structure of an alphabetaT cell receptor. Proc Natl Acad Sci U S A. 1999; 96:1547–1552. [PubMed: 9990061]
9. Grakoui A, Bromley SK, Sumen C, Davis MM, Shaw AS, Allen PM, Dustin ML. The immunological synapse: a molecular machine controlling T cell activation. Science. 1999; 285:221–227. [PubMed: 10398592]
10. Minguet S, Swamy M, Alarcon B, Luescher IF, Schamel WW. Full activation of the T cell receptor requires both clustering and conformational changes at CD3. Immunity. 2007; 26:43–54. [PubMed: 17188005]
11. Schamel WW, Arechaga I, Risueno RM, van Santen HM, Cabezas P, Risco C, Valpuesta JM, Alarcon B. Coexistence of multivalent and monovalent TCRs explains high sensitivity and wide range of response. J Exp Med. 2005; 202:493–503. [PubMed: 16087711]
12. Huppa JB, Axmann M, Mortelmaier MA, Lillemeier BF, Newell EW, Brameshuber M, Klein LO, Schutz GJ, Davis MM. TCR-peptide-MHC interactions in situ show accelerated kinetics and increased affinity. Nature. 2010; 463:963–967. [PubMed: 20164930]
13. Kumar R, Ferez M, Swamy M, Arechaga I, Rejas MT, Valpuesta JM, Schamel WW, Alarcon B, van Santen HM. Increased sensitivity of antigen-experienced T cells through the enrichment of oligomeric T cell receptor complexes. Immunity. 2011; 35:375–387. [PubMed: 21903423]
14. Alivisatos P. The use of nanocrystals in biological detection. Nat Biotechnol. 2004; 22:47–52. [PubMed: 14704706]
15. Mattoussi H, Mauro JM, Goldman ER, Anderson GP, Sundar VC, Mikulec FV, Bawendi MG. Self-assembly of CdSe-ZnS quantum dot bioconjugates using an engineered recombinant protein. J Am Chem Soc. 2000; 122:12142–12150.
16. Boyle S, Kolin DL, Bieler JG, Schneck JP, Wiseman PW, Edidin M. Quantum dot fluorescence characterizes the nanoscale organization of T cell receptors for antigen. Biophys J. 2011; 101:L57–59. [PubMed: 22261075]
17. Lillemeier BF, Mortelmaier MA, Forstner MB, Huppa JB, Groves JT, Davis MM. TCR and Lat are expressed on separate protein islands on T cell membranes and concatenate during activation. Nat Immunol. 2010; 11:90–96. [PubMed: 20010844]
18. Bruchez M Jr. Moronne M, Gin P, Weiss S, Alivisatos AP. Semiconductor nanocrystals as fluorescent biological labels. Science. 1998; 281:2013–2016. [PubMed: 9748157]
19. Hotz CZ. Applications of quantum dots in biology: an overview. Methods Mol Biol. 2005; 303:1–17. [PubMed: 15923671]
20. Michalet X, Pinaud FF, Bentolila LA, Tsay JM, Doose S, Li JJ, Sundaresan G, Wu AM, Gambhir SS, Weiss S. Quantum dots for live cells, in vivo imaging, and diagnostics. Science. 2005; 307:538–544. [PubMed: 15681376]

21. Tanaka KA, Suzuki KG, Shirai YM, Shibutani ST, Miyahara MS, Tsuboi H, Yahara M, Yoshimura A, Mayor S, Fujiwara TK, Kusumi A. Membrane molecules mobile even after chemical fixation. Nat Methods. 2010; 7:865–866. [PubMed: 20881966]
22. Meuer SC, Hussey RE, Cantrell DA, Hodgdon JC, Schlossman SF, Smith KA, Reinherz EL. Triggering of the T3-Ti antigen-receptor complex results in clonal T-cell proliferation through an interleukin 2-dependent autocrine pathway. Proc Natl Acad Sci U S A. 1984; 81:1509–1513. [PubMed: 6231642]
23. Van Wauwe JP, De Mey JR, Goossens JG. OKT3: a monoclonal anti-human T lymphocyte antibody with potent mitogenic properties. J Immunol. 1980; 124:2708–2713. [PubMed: 6966296]
24. Cho NH, Cheong TC, Min JH, Wu JH, Lee SJ, Kim D, Yang JS, Kim S, Kim YK, Seong SY. A multifunctional core-shell nanoparticle for dendritic cell-based cancer immunotherapy. Nat Nanotechnol. 2011; 6:675–682. [PubMed: 21909083]
25. Sun C, Lee JS, Zhang M. Magnetic nanoparticles in MR imaging and drug delivery. Adv Drug Deliv Rev. 2008; 60:1252–1265. [PubMed: 18558452]
26. Klippstein R, Pozo D. Nanotechnology-based manipulation of dendritic cells for enhanced immunotherapy strategies. Nanomedicine. 2010; 6:523–529. [PubMed: 20085824]
27. Hamdy S, Haddadi A, Shayeganpour A, Samuel J, Lavasanifar A. Activation of antigen-specific T cell-responses by mannan-decorated PLGA nanoparticles. Pharm Res. 2011; 28:2288–2301. [PubMed: 21560020]
28. Hirosue S, Kourtis IC, van der Vlies AJ, Hubbell JA, Swartz MA. Antigen delivery to dendritic cells by poly(propylene sulfide) nanoparticles with disulfide conjugated peptides: Cross-presentation and T cell activation. Vaccine. 2010; 28:7897–7906. [PubMed: 20934457]
29. Jewell CM, Lopez SC, Irvine DJ. In situ engineering of the lymph node microenvironment via intranodal injection of adjuvant-releasing polymer particles. Proc Natl Acad Sci U S A. 2011; 108:15745–15750. [PubMed: 21896725]
30. Nembrini C, Stano A, Dane KY, Ballester M, van der Vlies AJ, Marsland BJ, Swartz MA, Hubbell JA. Nanoparticle conjugation of antigen enhances cytotoxic T-cell responses in pulmonary vaccination. Proc Natl Acad Sci U S A. 2011; 108:E989–997. [PubMed: 21969597]
31. Pathak S, Davidson MC, Silva GA. Characterization of the functional binding properties of antibody conjugated quantum dots. Nano Lett. 2007; 7:1839–1845. [PubMed: 17536868]
32. Davis SJ, van der Merwe PA. The kinetic-segregation model: TCR triggering and beyond. Nat Immunol. 2006; 7:803–809. [PubMed: 16855606]
33. Maloney DG, Grillo-Lopez AJ, White CA, Bodkin D, Schilder RJ, Neidhart JA, Janakiraman N, Foon KA, Liles TM, Dallaire BK, Wey K, Royston I, Davis T, Levy R. IDEC-C2B8 (Rituximab) anti-CD20 monoclonal antibody therapy in patients with relapsed low-grade non-Hodgkin's lymphoma. Blood. 1997; 90:2188–2195. [PubMed: 9310469]
34. Anderson KC, Bates MP, Slaughenhoupt BL, Pinkus GS, Schlossman SF, Nadler LM. Expression of human B cell-associated antigens on leukemias and lymphomas: a model of human B cell differentiation. Blood. 1984; 63:1424–1433. [PubMed: 6609729]

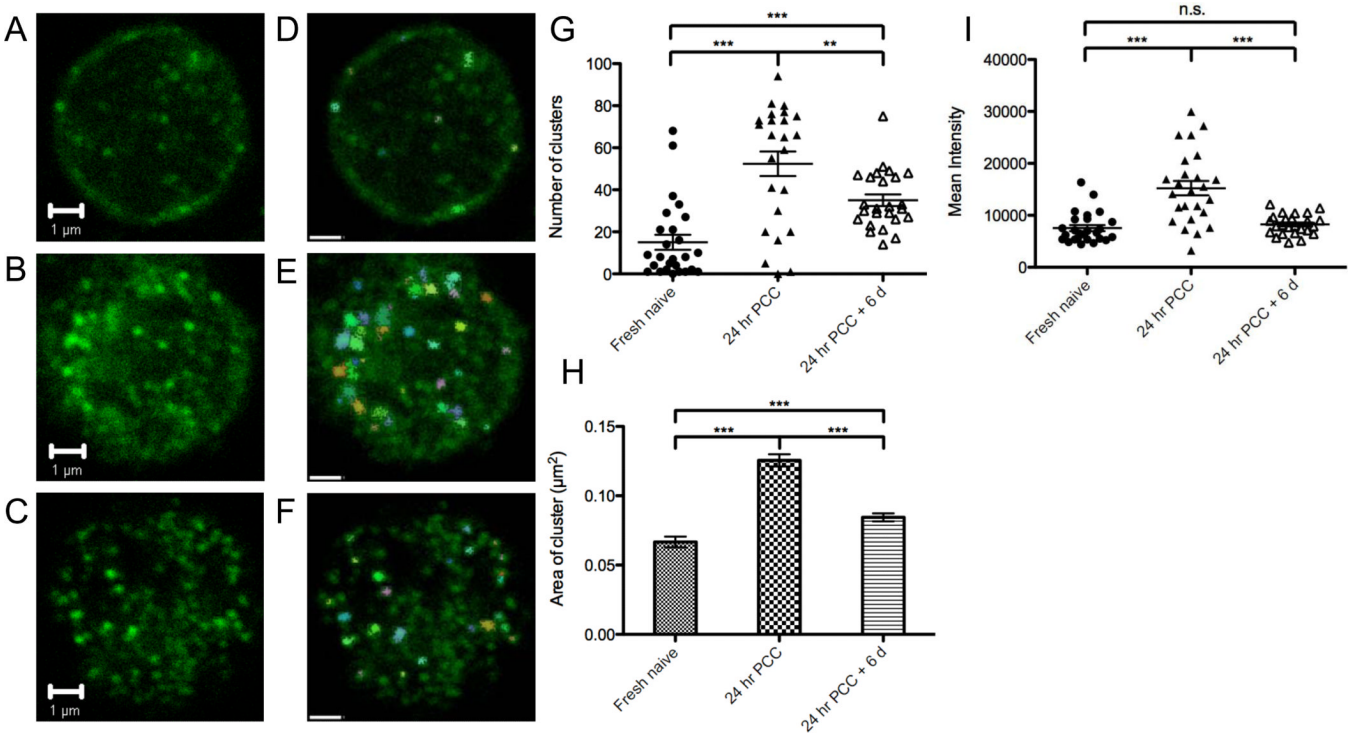

FIGURE 1.

Antigen stimulation induces TCR clustering. (**A**) Fresh naïve 5C.C7 splenocytes, (**B**) 5C.C7 splenocytes stimulated with 50 nM PCC for 24 hours, and (**C**) 5C.C7 splenocytes stimulated with 50 nM PCC for 24 hours, washed with PBS, and rested in 1 μg/ml IL-2 and IL-7 without PCC for another 6 days were fixed by 2% formaldehyde, stained for CD3, and imaged by confocal microscopy. (**D-F**) Microclusters were classified by size and size classes color-coded using Volocity imaging analysis software. Objects with area smaller then 0.01 μm^2 were excluded. The scale bars represent 1 μm. (**G**) The average number of microclusters identified on each cell ($n \geq 25$). (**H**) The average area of each microcluster. (**I**) The mean intensity of each cell ($n \geq 25$). ** and *** indicates $p < 0.01$ and $p < 0.001$ (two-tailed T-test). Data are representative of three independent experiments.

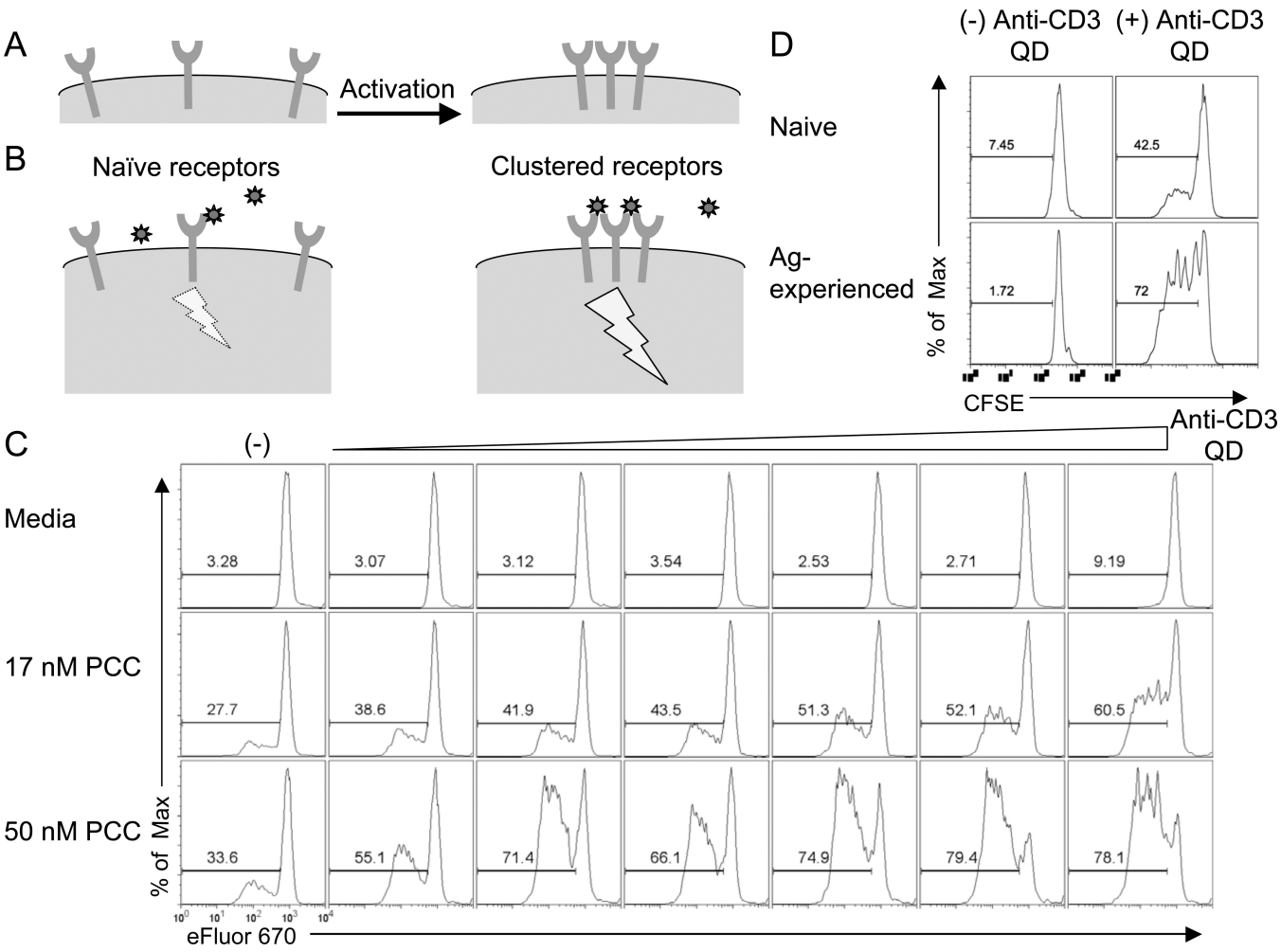

FIGURE 2.

Anti-CD3 QD activate antigen-experienced cells. (**A**) Receptors are mostly dispersed on the surface of a naïve T cell. Upon activation, receptors cluster. (**B**) The dispersed receptors are not readily crosslinked by binding of a ligand-coated nanoparticle and this interaction delivers a minimal signal. However, ligand-coated nanoparticles can bind multiple receptors in a cluster; this induces strong signaling. (**C**) eFluor 670 dilution in naïve 5C.C7 splenocytes stimulated for 3 days with 0, 17, or 50 nM PCC in combination with various concentration of anti-CD3 QD. (**D**) Naïve purified CD4+ 5C.C7 cells and antigen-experienced CD4+ 5C.C7 cells as shown in **Fig. 1C** were labeled with CFSE and incubated with irradiated APCs (in the absence of PCC) in the presence or absence of 1 nM anti-CD3 QD for 3 days. CFSE dilution measures cell proliferation. Data are representative of at least three independent experiments.

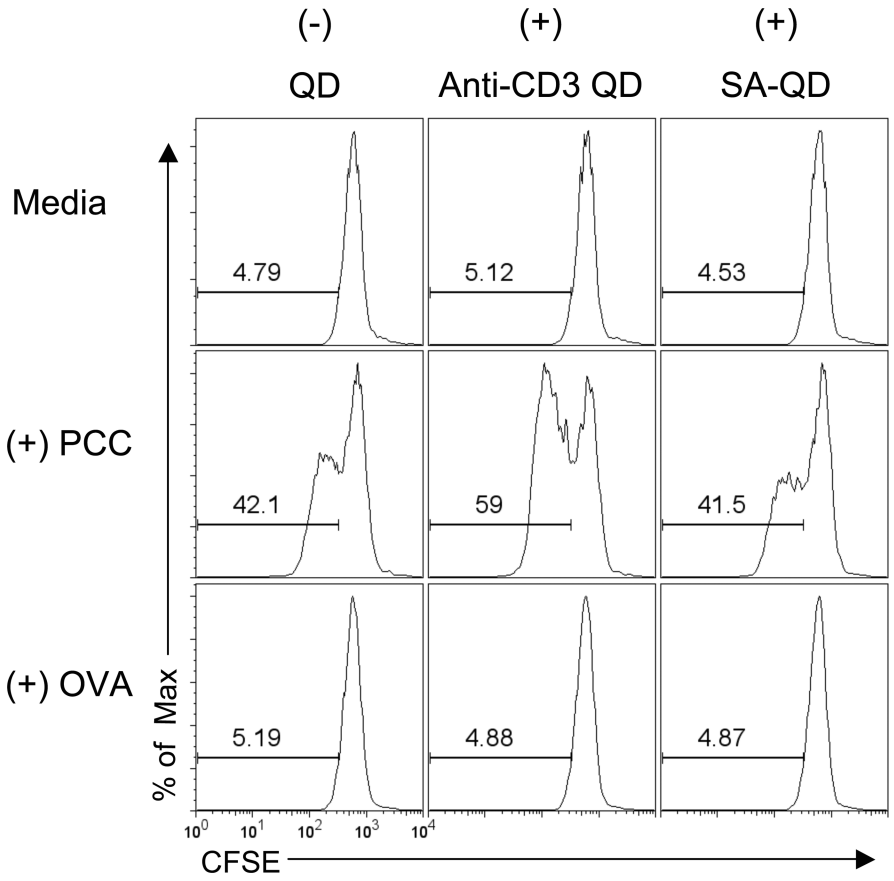

FIGURE 3.

CD4+ T cell activation by anti-CD3 QD is antigen-specific and does not occur with empty QD. CFSE dilution in naïve 5C.C7 splenocytes stimulated with no antigen, 50 nM PCC, or 50 nM OVA with or without 18.5 pM anti-CD3 QD, or 18.5 pM streptavidin QD for 3 days. Data are representative of three independent experiments.

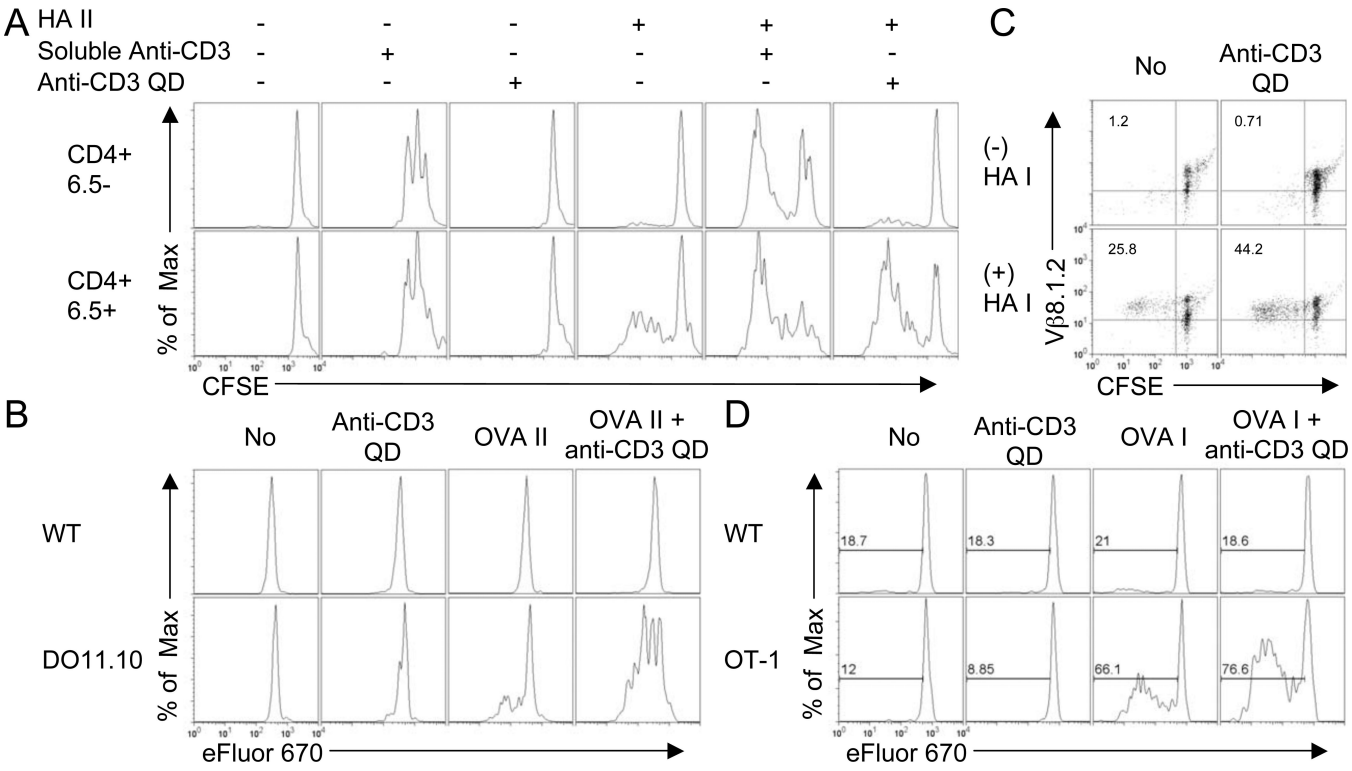

FIGURE 4.

Anti-CD3 QD promote selective, antigen-specific, activation of both CD4+ and CD8+ T cells. (**A**) Splenocytes from 6.5 TCR transgenic mice were stimulated with or without HA II peptide for 2 days followed by addition of media, soluble anti-CD3 antibody, or anti-CD3 QD and cultured for another 2 days. CFSE dilutions in CD4+ 6.5− gated T cells and CD4+ 6.5+ gated T cells from the same cultures are shown. (**B**) Splenocytes from DO11.10 RAG2−/− (Thy1.2) and wild type B10.D2 (Thy1.1) mice were mixed and stimulated with or without OVA II peptide for 1 day followed by addition of media or anti-CD3 QD for another 2 day culture. eFluor 670 dilutions in wild type, CD4+ Thy1.1+ gated, and DO11.10, CD4+ Thy1.2+ gated, cells from the same cultures are shown. (**C**) Splenocytes from Clone 4 TCR transgenic mice were stimulated with or without HA I peptide for 1 day followed by addition of media or anti-CD3 QD and cultured for another 2 days. CFSE dilutions versus CD8+ Vβ8.1.2+ population are shown. (**D**) Splenocytes from OT-1 RAG2−/− (Thy1.1) and wild type C57BL/6 (Thy1.2) mice were mixed and stimulated with or without OVA I peptide for 1 day followed by addition of media or anti-CD3 QD and cultured for another 2 days. eFluor 670 dilutions in wild type (CD8+ Thy1.2+ gated) and OT-1 (CD4+ Thy1.1+ gated) cells from the same cultures are shown. Data are representative of three independent experiments.

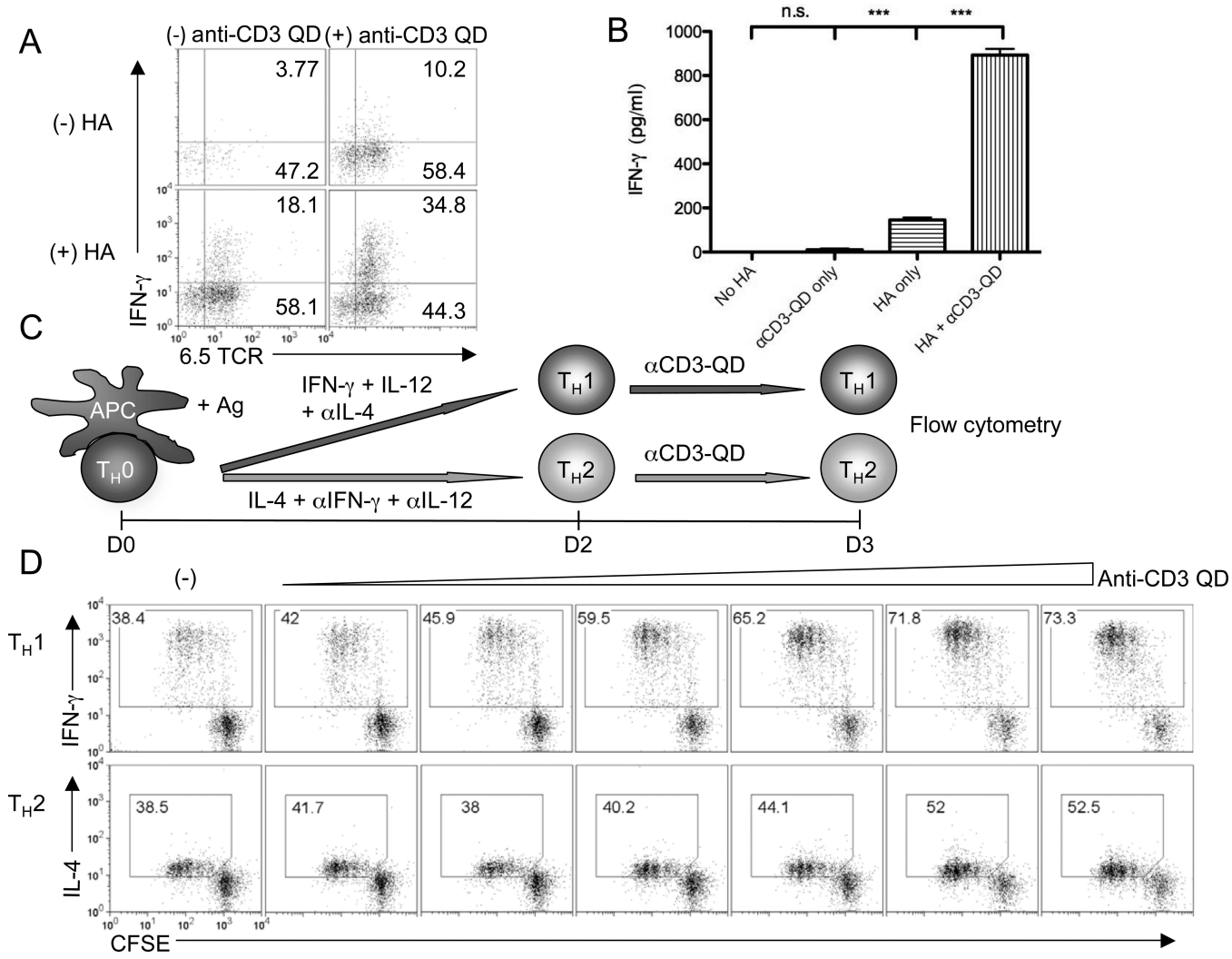

FIGURE 5.

Anti-CD3 QD enhance cytokine production. (**A**) IFN-γ production in 6.5 splenocytes stimulated with or without HA II peptide for 2 days, followed by another 4-day culture with or without the presence of anti-CD3 QD. CD4+ gated cells were shown. (**B**) IFN-γ production by 6.5 splenocytes. Data are representative of three independent experiments. (**C**) Schematic representation of experiment setup. Naïve 5C.C7 splenocytes were CFSE labeled and stimulated with PCC in T_H1- or T_H2-skewing conditions for 2 days followed by boosting with various concentration of anti-CD3 QD for 1 more day. (**D**) CFSE dilution and cytokine production of 5C.C7 CD4+ T cells labeled, skewed, and boosted as in **C**. *** indicates $p < 0.001$ (two-tailed T-test). Data are representative of three independent experiments.

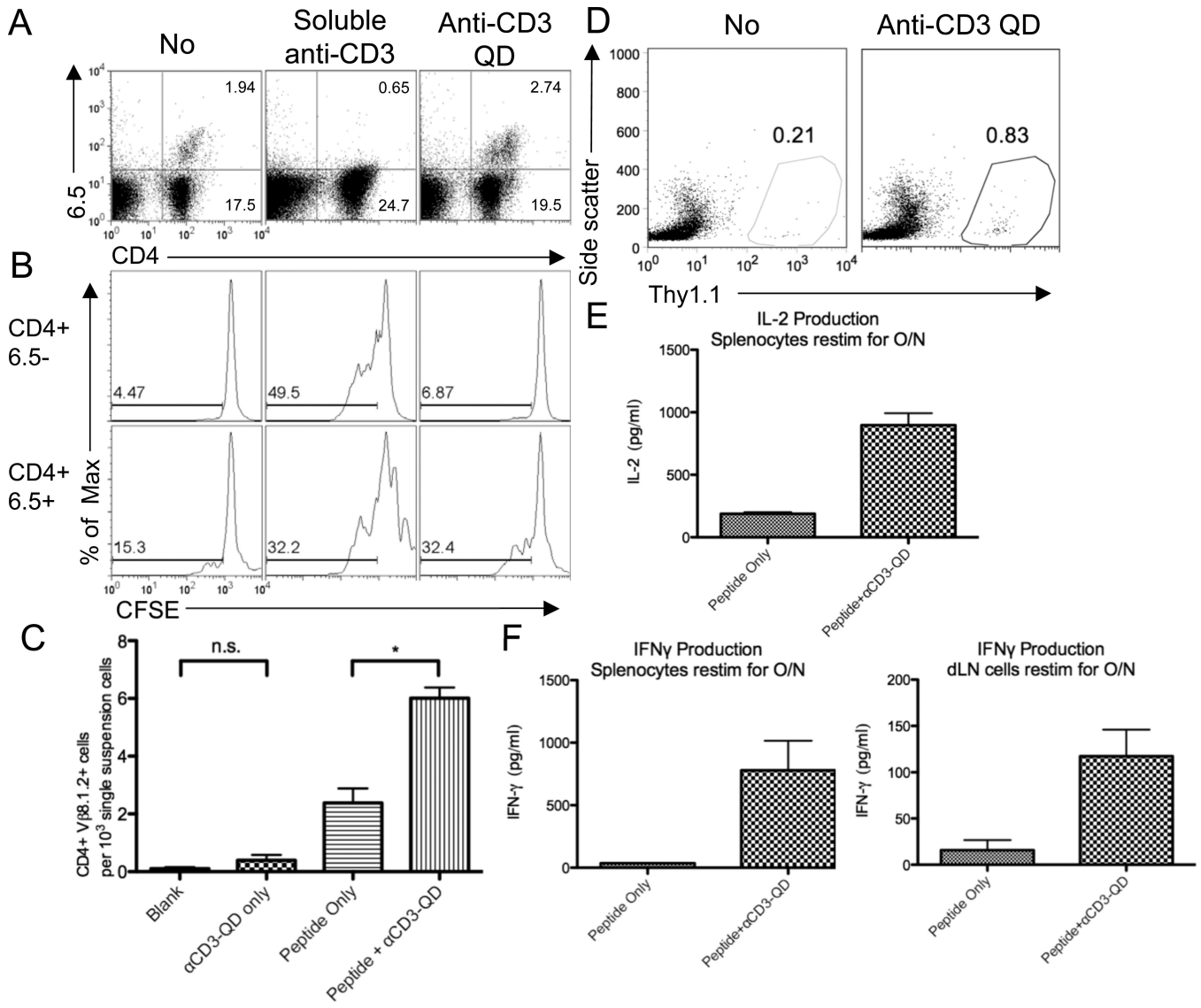

FIGURE 6.

Anti-CD3 QD boost antigen-specific responses of T cells stimulated *in vivo*. (**A**) CD4+ 6.5 splenocytes were transferred to recipient B10.D2 mice. The recipients were immunized subcutaneously with HA II peptide and CFA. Single cell suspensions of draining lymph nodes obtained 6 days after vaccination were CFSE labeled and rechallenged with media, soluble anti-CD3, or anti-CD3 QD for another 2 days. Recovery of antigen-specific CD4+ 6.5+ cells is shown. (**B**) CFSE dilutions in CD4+ 6.5− gated cells and CD4+ 6.5+ gated cells from the same cultures were shown. Note, the decreased percentage of 6.5+ T cells in the cultures treated with soluble anti-CD3 is due to the relative increase in 6.5− T cells in response to this non-specific stimulus. (**C**) Proportion of CD4+ Vβ8.1.2+ cells in single cell suspensions of draining lymph nodes from B10.D2 (Thy1.2) mice given adoptive transfer of CD4+ 6.5 splenocytes (Thy1.1) and immunized as in **A** or with PBS 2 days prior to subcutaneous boost with media or anti-CD3 QD; single cell suspensions of draining lymph nodes were obtained 3 days after boost. (**D**) B10.D2 mice were given adoptive transfer and immunized as in **A** 1 day prior to subcutaneous boost with media or anti-CD3 QD. Mice were rechallenged with Vaccinia-HA at Day 11. Recovery of adoptively transferred cells at

Day 14 is shown as Thy1.1+ cells. (**E**) IL-2 and (**F**) IFN-γ production by splenocytes and cells from draining lymph nodes from **D** stimulated with HA-II peptide for overnight. * indicates $p < 0.05$ (two-tailed T-test). Data are representative of three (**A-C**) or two (**D-F**) independent experiments.